

of *trans*-MoH<sub>2</sub>(DPE)<sub>2</sub> (3) and 0.010 g of a brownish yellow complex. The structure of the latter complex is yet uncertain. *Anal.* Found: C, 64.86; H, 5.44; Cl, 9.51.

#### Reactions of Molybdenum Hydride Complexes with Nitrogen.

(1) **Reaction of the Hydride Complex 3 with Nitrogen.** Nitrogen gas was bubbled into a stirred solution of 0.075 g (0.083 mmol) of *trans*-MoH<sub>2</sub>(DPE)<sub>2</sub> (3) in 15 ml of benzene at ambient temperature for 3 days. After addition of 10 ml of *n*-hexane, yellow crystals of the unreacted hydride complex 3 were precipitated. The crystals were filtered off and the filtrate was concentrated to a volume of ca 5 ml under a reduced pressure. Addition of 5 ml of *n*-hexane to the solution gave *trans*-Mo(N<sub>2</sub>)<sub>2</sub>(DPE)<sub>2</sub> (2) as orange crystals, yield 0.010 g (13%).

(2) **Reaction of the Hydride Complex 4 with Nitrogen.** The reaction was carried out as above, except that toluene was used as the solvent instead of benzene. Most of the hydride complex remained unreacted, but a small amount of *trans*-Mo(N<sub>2</sub>)<sub>2</sub>(DPE)<sub>2</sub> (2) was obtained, yield 11%.

**Reaction of the Bis(dinitrogen) Complex 2 with Trihydridotris(triphenylphosphine)cobalt(III).** (1) **Reaction in Benzene.** To a stirred solution of 0.119 g (0.125 mmol) of *trans*-Mo(N<sub>2</sub>)<sub>2</sub>(DPE)<sub>2</sub> (2) in 6 ml of benzene was added a solution of 0.120 g (0.142 mmol) of CoH<sub>3</sub>(PPh<sub>3</sub>)<sub>3</sub> in 6 ml of benzene at ambient temperature under argon. The reaction mixture turned gradually dark. A small amount of dark brown solid precipitated with evolution of nitrogen and hydrogen gas. The mixture was stirred for 3 days. The infrared spectrum of the solution showed two bands at 2088 and 1980 cm<sup>-1</sup> assignable to the N-N stretching frequencies of CoH(N<sub>2</sub>)(PPh<sub>3</sub>)<sub>3</sub> and *trans*-Mo(N<sub>2</sub>)<sub>2</sub>(DPE)<sub>2</sub> (2), respectively. After removal of the dark brown precipitate by filtration, 10 ml of *n*-hexane was added to the filtrate. Then yellow crystals were deposited in addition to a small amount of orange crystals of the unreacted N<sub>2</sub> complex 2. The yellow complex was recrystallized from benzene-*n*-hexane, giving the pure hydride complex *trans*-MoH<sub>2</sub>(DPE)<sub>2</sub> (3) as yellow crystals, yield 0.020 g (18%). *Anal.* Calcd for C<sub>32</sub>H<sub>50</sub>P<sub>4</sub>Mo: C, 69.80; H, 5.63; N, 0. Found: C, 69.53; H, 6.15; N, 0.0. However, the dinitrogen-cobalt complex CoH(N<sub>2</sub>)(PPh<sub>3</sub>)<sub>3</sub> could not be isolated from the solution.

(2) **Reaction in Toluene.** The reaction was carried out as above, except that toluene was used instead of benzene as the solvent. The infrared spectrum of the mixture showed the formation of the dinitrogen-cobalt complex CoH(N<sub>2</sub>)(PPh<sub>3</sub>)<sub>3</sub>, but the complex was not isolated. However, the hydride complex [*trans*-MoH<sub>2</sub>(DPE)]<sub>2</sub>-μ-(DPE) (4) was isolated from the solution, yield 25%.

**Reactions of Dinitrogen-Molybdenum Complexes with Carbon Monoxide.** (1) **Reaction of the Dinitrogen-Molybdenum Complex**

**1 with Carbon Monoxide.** Through a stirred suspension of 0.314 g of Mo(N<sub>2</sub>)(PPh<sub>3</sub>)<sub>2</sub>·C<sub>6</sub>H<sub>5</sub>CH<sub>3</sub> (1) in 80 ml of toluene was bubbled carbon monoxide at ambient temperature for 17 days. The mixture turned gradually red and became almost homogeneous. The unreacted N<sub>2</sub> complex 1 was filtered off and the red filtrate was concentrated to a volume of ca. 25 ml under a reduced pressure. Addition of 25 ml of *n*-hexane to the solution deposited orange crystals, which were filtered, washed several times with *n*-hexane, and dried *in vacuo*, yield 0.150 g (55%). *Anal.* Calcd for C<sub>37</sub>H<sub>30</sub>OP<sub>2</sub>Mo: C, 68.52; H, 4.66; N, 0. Found: C, 67.17; H, 4.77; N, 0.0.

(2) **Reaction of the Bis(dinitrogen) Complex 2 with Carbon Monoxide.** Through a stirred solution of 0.120 g (0.126 mmol) of *trans*-Mo(N<sub>2</sub>)(DPE)<sub>2</sub> (2) in 15 ml of toluene was bubbled carbon monoxide at ambient temperature for 4 days. Addition of 15 ml of methanol to the solution gave pale yellow crystals as well as the unreacted bis(dinitrogen) complex 2. The pale yellow complex was washed several times with methanol and dried *in vacuo*, yield 0.025 g (21%). *Anal.* Calcd for C<sub>34</sub>H<sub>48</sub>O<sub>2</sub>P<sub>4</sub>Mo: C, 68.36; H, 5.10; N, 0. Found: C, 68.63; H, 5.27; N, 0.0.

The infrared spectrum of the pale yellow complex showed two strong bands at 1855 and 1785 cm<sup>-1</sup> assignable to ν<sub>C=O</sub> (lit.<sup>21</sup> 1852 and 1786 cm<sup>-1</sup>).

**Preparation of *trans*-Tetracarbonylbis(triphenylphosphine)molybdenum(0) and *cis*-Dicarbonyltetrakis(triphenylphosphine)molybdenum(0).** To a stirred solution of 0.723 g (1.84 mmol) of molybdenum(III) acetylacetonate and 4.840 g (18.4 mmol) of triphenylphosphine in 35 ml of toluene was added 2.2 g (11.1 mmol) of triisobutylaluminum at -40° under argon. The temperature was gradually raised to ambient temperature and carbon monoxide was bubbled into the reaction mixture for 30 min at that temperature. Addition of 30 ml of *n*-hexane to the solution gave *cis*-Mo(CO)<sub>2</sub>(PPh<sub>3</sub>)<sub>4</sub> as brownish yellow crystals. The complex was filtered, washed with *n*-hexane, and dried *in vacuo*, yield 0.02 g (0.9%). *Anal.* Calcd for C<sub>74</sub>H<sub>60</sub>O<sub>2</sub>P<sub>4</sub>Mo: C, 74.00; H, 5.04. Found: C, 73.40; H, 5.48.

The filtrate was concentrated under reduced pressure to a volume of 30 ml. Addition of 20 ml of *n*-hexane to the solution gave *trans*-Mo(CO)<sub>2</sub>(PPh<sub>3</sub>)<sub>2</sub> as a pale yellow solid. The complex was washed with *n*-hexane and dried *in vacuo*, yield 0.120 g (8.9%). *Anal.* Calcd for C<sub>46</sub>H<sub>30</sub>O<sub>4</sub>P<sub>2</sub>Mo: C, 65.56; H, 4.13. Found: C, 65.31; H, 4.51.

(21) J. Chatt and H. R. Watson, *J. Chem. Soc.*, 4980 (1961).

## The Structure of the 7,7'-*commo*-Bis[dodecahydro-7-nickela-*nido*-undecaborate] Dianion

L. J. Guggenberger

Contribution No. 1730 from the Central Research Department, Experimental Station, E. I. du Pont de Nemours and Company, Wilmington, Delaware 19898. Received May 13, 1971

**Abstract:** The crystal structure of tetramethylammonium 7,7'-*commo*-bis[dodecahydro-7-nickela-*nido*-undecaborate](2-), [(CH<sub>3</sub>)<sub>4</sub>N]<sub>2</sub>Ni(B<sub>10</sub>H<sub>12</sub>)<sub>2</sub>, was determined by single crystal X-ray techniques. Crystals are monoclinic, space group P2<sub>1</sub>/c, with *a* = 7.34 (1), *b* = 11.97 (2), *c* = 15.73 (2) Å, and β = 93.8 (1)°. There are two formula units per cell with observed and calculated densities of 1.09 g/cm<sup>3</sup>. The structure was refined by least-squares to an *R* of 0.096. The anion has C<sub>2</sub>( $\bar{1}$ ) space group imposed molecular symmetry. The nickel atom bonds to eight boron atoms and fuses two 11-atom polyhedral fragments giving two chemically different Ni-B distances of 2.23 and 2.15 Å. All the hydrogen atoms were located and refined. The two nonterminal hydrogen atoms bridge edge positions of the open pentagonal faces of the borane polyhedron. Extended Hückel molecular orbital calculations on the Ni(B<sub>10</sub>H<sub>12</sub>)<sub>2</sub> dianion show that the primary metal bonding comes from the 4s atomic orbital of nickel.

A variety of transition metal derivatives of B<sub>10</sub>H<sub>12</sub><sup>2-</sup> have been prepared recently.<sup>1</sup> Complexes reported

(1) F. Klanberg, P. A. Wegner, G. W. Parshall, and E. L. Muetterties, *Inorg. Chem.*, 7, 2072 (1968).

are of the type M(B<sub>10</sub>H<sub>12</sub>)<sub>2</sub><sup>2-</sup> (M = Co, Ni, Pd, Pt), M(B<sub>10</sub>H<sub>12</sub>)(PR<sub>3</sub>)<sub>2</sub> (M = Pd, Pt), and M(B<sub>10</sub>H<sub>12</sub>)L<sub>3</sub><sup>-</sup> (M = Co, Rh, Ir). Greenwood and Travers have also reported M(B<sub>10</sub>H<sub>12</sub>)<sub>2</sub><sup>2-</sup> complexes of zinc, cadmium,

and mercury.<sup>2-5</sup> Several types of interactions between the transition metal and the decaborane cage with the metal atom as a part of both cages fusing the borane cages have been postulated.<sup>1-5</sup>

This work reports the results of an X-ray crystal structure analysis of tetramethylammonium 7,7'-*commo*-bis[dodecahydro-7-nickela-*nido*-undecaborate](2-),  $[(\text{CH}_3)_4\text{N}]_2\text{Ni}(\text{B}_{10}\text{H}_{12})_2$ .<sup>6</sup> The resultant metal-borane configuration serves as a model for many of the transition metal  $\text{B}_{10}\text{H}_{12}^{2-}$  complexes.

### Experimental Section

Crystal data were examined for the diamagnetic nickel and paramagnetic cobalt complexes of  $\text{B}_{10}\text{H}_{12}^{2-}$ . Crystals of  $[(\text{CH}_3)_4\text{N}]_2\text{Ni}(\text{B}_{10}\text{H}_{12})_2$  are monoclinic with  $a = 7.34$  (1),  $b = 11.97$  (2),  $c = 15.73$  (2) Å, and  $\beta = 93.8$  (1)°. Crystals of  $[(\text{CH}_3)_4\text{N}]_2\text{Co}(\text{B}_{10}\text{H}_{12})_2$  are monoclinic with  $a = 7.341$  (4),  $b = 12.005$  (5),  $c = 15.785$  (4) Å, and  $\beta = 93.69$  (4)°. These cell parameters resulted from a least-squares refinement of powder data recorded on a Hägg-Guinier camera using a KCl internal standard ( $a_{25^\circ} = 6.2931$  Å). The systematic absences of  $h0l$ ,  $l = 2n + 1$ , and  $0k0$ ,  $k = 2n + 1$  uniquely establish the space group as  $P2_1/c$  for both complexes. The nickel and cobalt complexes are clearly isomorphous. The observed and calculated densities for two formula units per cell for  $[(\text{CH}_3)_4\text{N}]_2\text{Ni}(\text{B}_{10}\text{H}_{12})_2$  are both 1.09 g/cm<sup>3</sup>. The  $\text{Ni}(\text{B}_{10}\text{H}_{12})_2$  dianion has  $C_i(\bar{1})$  space group imposed molecular symmetry in the absence of disorder. All atoms are in the general space group positions 4e except the nickel atom which is at the origin of the cell.<sup>7</sup>

The nickel complex was chosen for this investigation because better crystals were available. The crystal chosen was a platelet of dimensions  $0.18 \times 0.18 \times 0.07$  mm. The data were collected on a Picker four-circle automatic diffractometer with the crystal mounted with the  $b^*$  axis coincident with the diffractometer  $\phi$  axis. The data were measured (1371 reflections) with Zr-filtered  $\text{Mo K}\alpha$  ( $\lambda$  0.7107 Å) radiation. The  $\theta$ - $2\theta$  scan technique was used with a scan speed of 1°/min and a scan range of 1.5° plus the  $\text{K}\alpha_1$ - $\text{K}\alpha_2$  angular separation. Individual backgrounds of 20 sec were recorded before and after each scan.

The data were corrected for Lorentz, polarization, and absorption effects. The crystal was approximated by six plane faces in applying the absorption correction. The linear absorption coefficient for  $\text{Mo K}\alpha$  radiation is 7.1 cm<sup>-1</sup>. The calculated transmission factors varied from 0.86 to 0.96. Structure factors which were less than their estimated standard deviations<sup>8</sup> were called "unobserved" and given zero weight in the refinement.

The structure was solved by heavy-atom techniques, namely, phasing electron density maps with the nickel atom and then in three steps adding further atoms to the structure factor calculation. A calculation with anisotropic thermal parameters for the nickel atom and isotropic thermal parameters for the remaining nonhydrogen atoms gave an  $R$  value ( $\sum ||F_o| - |F_c|| / \sum |F_o|$ ) of 0.127. Two least-squares cycles with anisotropic thermal parameters for all nonhydrogen atoms reduced the  $R$  to 0.113. The  $hk0$  and  $\bar{h}k0$  data, equivalent in the  $P2_1/c$  symmetry group, were both collected initially and averaged at this point. All the hydrogen atoms on the metalloborane dianion were located on an electron density difference map. The hydrogen atom positional parameters were refined but not the isotropic thermal parameters which were set at 4.0 Å<sup>2</sup>. The refinement converged after several more least-squares cycles with a final  $R$  of 0.096 and  $wR(\{\sum w(|F_o| - |F_c|)^2 / \sum w|F_o|^2\}^{1/2})$  of 0.078. The standard deviation of an observation of unit weight for 1056 pieces of data and 178 variables was 1.81. This is somewhat large and implies that the estimated errors in the structure factors may have been underestimated, but it may be

**Table I.** Final Positional Parameters for  $[(\text{CH}_3)_4\text{N}]_2\text{Ni}(\text{B}_{10}\text{H}_{12})_2^a$

Atom	x	y	z
Ni	0	0	0
N	0.4500 (12)	-0.0168 (9)	0.2957 (5)
C(1)	0.5371 (23)	0.0202 (16)	0.3814 (9)
C(2)	0.2755 (27)	-0.0550 (21)	0.3139 (13)
C(3)	0.5357 (31)	-0.1127 (17)	0.2631 (10)
C(4)	0.4123 (29)	0.0654 (12)	0.2290 (9)
B(1)	0.0365 (21)	-0.2429 (13)	0.1011 (9)
B(2)	-0.2052 (19)	-0.2164 (10)	0.0870 (9)
B(3)	-0.1016 (20)	-0.3090 (12)	0.0169 (9)
B(4)	0.1293 (19)	-0.2674 (11)	0.0018 (9)
B(5)	-0.0487 (16)	-0.1011 (11)	0.1057 (8)
B(6)	-0.2515 (19)	-0.0837 (12)	0.0415 (8)
B(7)	-0.2714 (18)	-0.2130 (12)	-0.0213 (8)
B(8)	-0.0482 (23)	-0.2497 (15)	-0.0789 (10)
B(9)	0.1314 (19)	-0.1450 (11)	-0.0587 (9)
B(10)	0.1654 (16)	-0.1375 (10)	0.0535 (7)
H(1)	0.073 (13)	-0.275 (9)	0.160 (6)
H(2)	-0.306 (13)	-0.256 (9)	0.128 (6)
H(3)	-0.131 (13)	-0.403 (9)	0.007 (6)
H(4)	0.249 (12)	-0.357 (8)	-0.009 (6)
H(5)	-0.021 (13)	-0.044 (7)	0.167 (6)
H(6)	-0.385 (13)	-0.030 (8)	0.053 (6)
H(7)	-0.405 (13)	-0.232 (9)	-0.046 (6)
H(8)	-0.080 (13)	-0.292 (9)	-0.146 (7)
H(9)	0.254 (12)	-0.140 (9)	-0.109 (6)
H(10)	0.357 (12)	-0.084 (8)	0.078 (6)
H(67)	-0.288 (14)	-0.076 (9)	-0.026 (7)
H(89)	-0.019 (15)	-0.145 (10)	-0.107 (7)

<sup>a</sup> The standard deviations of the least significant digits are in parentheses. The numbering system is illustrated in Figure 1.

due in part to some inadequacy in the refinement of the cation atom positions. A few of the hydrogen atom positional shifts in the last refinement cycle were nearly as large as their standard deviations so that accumulated shifts in these parameters in further refinements could exceed their estimated standard deviations. The large thermal motion of the methyl carbon atoms prohibited the location of their hydrogen atoms.

Atomic scattering factors for the neutral atoms were used.<sup>9</sup> The real and imaginary parts of the anomalous scattering effect were included for the nickel atom.<sup>10</sup> The refinement minimized the function  $\sum w|F_o| - |F_c|^2$ .<sup>11</sup>

### Results and Discussion

The final positional parameters are given in Table I and the thermal parameters in Table II. A table of the observed and calculated structure factors ( $\times 10$ ) is available.<sup>12</sup>

The structure of the metalloborane anion,  $\text{Ni}(\text{B}_{10}\text{H}_{12})_2^{2-}$ , is shown in Figure 1. Hydrogen atoms are identified by the boron atoms to which they are attached; thus, H(67) is the hydrogen atom bridging B(6) and B(7), etc. The nickel atom occupies the fifth position in the open pentagonal face of both borane cages and serves to fuse the two 11-atom polyhedral frameworks. The anion has  $C_i(\bar{1})$  symmetry where the cage

(9) H. P. Hanson, F. Herman, J. D. Lea, and S. Skillman, *Acta Crystallogr.*, **17**, 1040 (1964).

(10) D. H. Templeton, "International Tables for X-ray Crystallography," Vol. III, The Kynoch Press, Birmingham, England, 1962, p 215.

(11) Computer programs used, in addition to various local programs, were Prewitt's least-squares program SFLS5 and absorption correction program ACACA, the Busing-Lévy error function program ORFFE, the Fourier program FOUR written originally by C. J. Fritchie, Jr., and the Johnson plotting program ORTEP.

(12) Listings of the observed and calculated structure factors will appear following these pages in the microfilm edition of this volume of the journal. Single copies may be obtained from the Reprint Department, ACS Publications, 1155 Sixteenth St., N.W., Washington, D. C. 20036, by referring to author, title of article, volume, and page number. Remit check or money order for \$3.00 for photocopy or \$2.00 for microfiche.

(2) N. N. Greenwood and N. F. Travers, *J. Chem. Soc. A*, 15 (1968).

(3) N. N. Greenwood and N. F. Travers, *ibid.*, 880 (1967).

(4) N. N. Greenwood and D. N. Sharrocks, *ibid.*, 2334 (1969).

(5) N. N. Greenwood and N. F. Travers, *Chem. Commun.*, 216 (1967).

(6) This is the recommended nomenclature for two fused undecaborane polyhedra. The atom numbering system used throughout this work was more conveniently chosen in terms of the decaborane ligand numbering system. See *Inorg. Chem.*, **7**, 1945 (1968), for nomenclature rules.

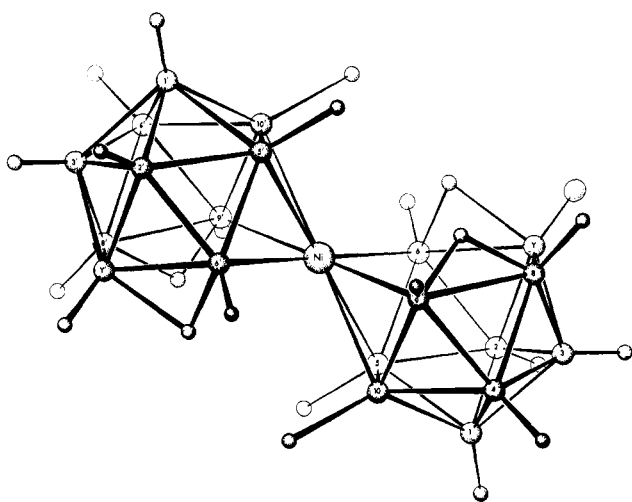
(7) "International Tables for X-ray Crystallography," Vol. I, The Kynoch Press, Birmingham, England, 1965, p 99.

(8) L. J. Guggenberger, *Inorg. Chem.*, **7**, 2260 (1968).

**Table II.** Final Thermal Parameters ( $\times 10^4$ ) for  $[(\text{CH}_3)_4\text{N}]_2\text{Ni}(\text{B}_{10}\text{H}_{12})_2^{2-}$ 

Atom	$\beta_{11}$	$\beta_{22}$	$\beta_{33}$	$\beta_{12}$	$\beta_{13}$	$\beta_{23}$
Ni	122 (3)	60 (2)	32 (1)	2 (4)	14 (1)	-1 (2)
N	302 (23)	70 (9)	33 (4)	-16 (16)	28 (8)	-14 (6)
C(1)	798 (63)	171 (22)	88 (9)	16 (34)	-80 (19)	-2 (14)
C(2)	654 (64)	589 (60)	141 (15)	-481 (53)	54 (26)	16 (23)
C(3)	1345 (108)	312 (29)	77 (11)	560 (50)	-81 (27)	-84 (15)
C(4)	1264 (104)	107 (15)	56 (9)	-13 (30)	-40 (23)	43 (9)
B(1)	229 (38)	91 (15)	23 (7)	54 (21)	16 (13)	-4 (9)
B(2)	258 (37)	44 (12)	59 (8)	-40 (18)	47 (15)	0 (8)
B(3)	274 (38)	26 (11)	51 (8)	17 (18)	23 (15)	13 (8)
B(4)	180 (34)	49 (13)	44 (8)	-37 (18)	32 (13)	-10 (8)
B(5)	112 (29)	67 (13)	43 (7)	-3 (16)	17 (12)	4 (8)
B(6)	156 (32)	90 (14)	38 (7)	-46 (18)	34 (13)	-8 (9)
B(7)	168 (31)	84 (14)	46 (7)	-33 (19)	47 (13)	-11 (8)
B(8)	298 (46)	102 (17)	37 (8)	17 (25)	6 (16)	-11 (10)
B(9)	142 (31)	47 (11)	52 (8)	19 (17)	19 (14)	3 (8)
B(10)	173 (30)	55 (11)	28 (6)	12 (16)	36 (11)	8 (7)

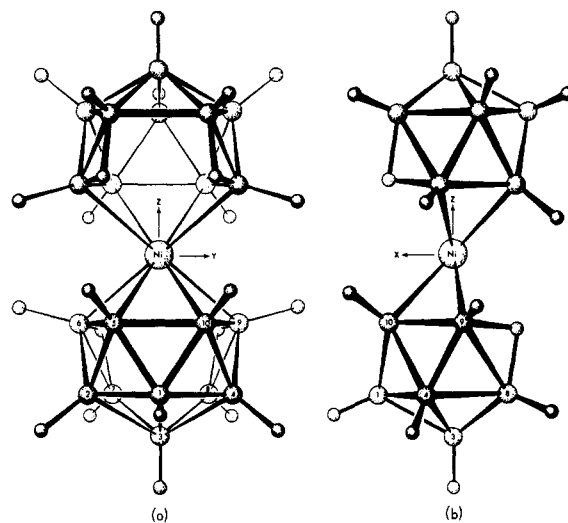
<sup>a</sup> The standard deviations of the least significant digits are given in parentheses. The anisotropic thermal ellipsoid is of the form  $\exp[-(\beta_{11}h^2 + \beta_{22}k^2 + \beta_{33}l^2 + 2\beta_{12}hk + 2\beta_{13}hl + 2\beta_{23}kl)]$ . The hydrogen atoms were assigned fixed isotropic temperature factors of  $4.0 \text{ \AA}^2$ .

Figure 1. The configuration of  $\text{Ni}(\text{B}_{10}\text{H}_{12})_2^{2-}$ .**Table III.** Bonding Interatomic Distances for  $[(\text{CH}_3)_4\text{N}]_2\text{Ni}(\text{B}_{10}\text{H}_{12})_2^{2-}$ 

Ni-B(5)	2.11 (1)	N-C(1)	1.52 (2)
Ni-B(6)	2.24 (1)	N-C(2)	1.41 (2)
Ni-B(9)	2.22 (1)	N-C(3)	1.42 (2)
Ni-B(10)	2.18 (1)	N-C(4)	1.45 (2)
B(1)-B(2)	1.80 (2)	B(1)-H(1)	1.03 (10)
B(1)-B(3)	1.80 (2)	B(2)-H(2)	1.12 (10)
B(1)-B(4)	1.77 (2)	B(3)-H(3)	1.16 (11)
B(1)-B(5)	1.81 (2)	B(4)-H(4)	1.41 (9)
B(1)-B(10)	1.77 (2)	B(5)-H(5)	1.19 (9)
B(2)-B(3)	1.77 (2)	B(6)-H(6)	1.20 (9)
B(2)-B(5)	1.81 (2)	B(7)-H(7)	1.06 (9)
B(2)-B(6)	1.77 (2)	B(8)-H(8)	1.19 (10)
B(2)-B(7)	1.74 (2)	B(9)-H(9)	1.24 (9)
B(3)-B(4)	1.80 (2)	B(10)-H(10)	1.57 (9)
B(3)-B(7)	1.77 (2)	B(6)-H(67)	1.08 (10)
B(3)-B(8)	1.73 (2)	B(7)-H(67)	1.64 (11)
B(4)-B(8)	1.77 (2)	B(8)-H(89)	1.35 (11)
B(4)-B(9)	1.75 (2)	B(9)-H(89)	1.30 (10)
B(4)-B(10)	1.77 (2)		
B(5)-B(6)	1.75 (2)		
B(5)-B(10)	1.87 (2)		
B(6)-B(7)	1.84 (2)		
B(7)-B(8)	1.97 (2)		
B(8)-B(9)	1.83 (2)		
B(9)-B(10)	1.77 (2)		

<sup>a</sup> The estimated standard deviations of the least significant figures are given in parentheses.

on the left of Figure 1 (primed atoms) is related to that on the right by the center of inversion at the nickel

Figure 2. Front and side view of the  $\text{Ni}(\text{B}_{10}\text{H}_{12})_2^{2-}$  structure. The coordinate system is that used in the MO calculations.

atom. The anion very nearly possesses the idealized  $C_{2h}$  point symmetry (*vide infra*) where the idealized mirror plane contains atoms B(1), H(1), B(3), H(3), Ni, B(1'), H(1'), B(3'), and H(3').

Alternatively, the dianion structure might be viewed in terms of two decaborane(12) ligands complexing the nickel atom in "sandwich" fashion. This illustrates the analogy to the transition metal complexes of the dicarbollide ion,  $(\text{B}_9\text{C}_2\text{H}_{11})^{2-}$ .<sup>13</sup> This structure description is emphasized in Figure 2 where the coordinate system has been rotated for molecular orbital calculations (*vide infra*).

A selected set of interatomic distances is given in Table III. A set of angles between bonding nonhydrogen atoms is given in Table IV. The interatomic distances were not corrected for thermal motion. The cation distances in particular are affected by the motion of the methyl groups. However, neither the "riding model" nor the "independent motion model"<sup>14</sup> gave meaningful corrections to these distances. The uncorrected average N-C distance of  $1.45 \text{ \AA}$  is close to  $1.47 \text{ \AA}$  which is in the sum of the covalent radii,<sup>15</sup> but the

(13) A list of references to these structures is given in Table V.

(14) W. R. Busing and H. A. Levy, *Acta Crystallogr.*, **17**, 142 (1964).

(15) L. Pauling, "The Nature of the Chemical Bond," 3rd ed, Cornell University Press, Ithaca, N. Y., 1960, p 246.

Table IV. Bond Angles, Deg<sup>a</sup>

B(5)-Ni-B(6)	47.5 (5)	B(4)-B(8)-B(9)	58.0 (8)
B(5)-Ni-B(10)	51.8 (4)	Ni-B(9)-B(10)	65.2 (6)
B(6)-Ni-B(9)	99.3 (6)	B(4)-B(9)-B(8)	59.2 (8)
B(9)-Ni-B(10)	47.4 (5)	B(4)-B(9)-B(10)	60.3 (7)
B(6)-Ni-B(5')	132.5 (5)	Ni-B(10)-B(5)	62.1 (5)
B(6)-Ni-B(9')	80.7 (6)	Ni-B(10)-B(9)	67.4 (6)
B(6)-Ni-B(10')	90.1 (5)	B-B(10)-B (av of 3)	59.6 (3)
B(9)-Ni-B(5')	91.1 (5)	C(1)-N-C(2)	104.5 (12)
B(9)-Ni-B(6')	80.7 (6)	C(1)-N-C(3)	112.7 (12)
B(9)-Ni-B(10')	132.6 (5)	C(1)-N-C(4)	119.5 (12)
B-B(1)-B (av of 5)	60.4 (7)	C(2)-N-C(3)	104.0 (16)
B-B(2)-B (av of 5)	60.6 (7)	C(2)-N-C(4)	103.6 (14)
B-B(3)-B (av of 4)	59.7 (4)	C(3)-N-C(4)	110.7 (11)
B(7)-B(3)-B(8)	68.6 (8)		
B-B(4)-B (av of 5)	60.4 (7)		
B-B(5)-B (av of 3)	58.9 (7)		
Ni-B(5)-B(6)	70.1 (6)		
Ni-B(5)-B(10)	66.1 (5)		
Ni-B(6)-B(5)	62.3 (5)		
B(2)-B(6)-B(5)	61.8 (8)		
B(2)-B(6)-B(7)	57.7 (8)		
B(2)-B(7)-B(3)	60.6 (8)		
B(2)-B(7)-B(6)	59.1 (7)		
B(3)-B(7)-B(8)	54.8 (7)		
B(3)-B(8)-B(4)	61.7 (8)		
B(3)-B(8)-B(7)	56.6 (8)		

<sup>a</sup> The estimated standard deviations are given in parentheses. The averages of angles are taken where such averages are meaningful; the estimated errors for these were calculated according to  $(\Sigma(d_i - \bar{d})^2/n(n-1))^{1/2}$ , where  $d_i$  and  $\bar{d}$  are the distances and mean distance, respectively.

spread in the chemically equivalent distances reflects the very large thermal parameters of these atoms.

There are two types of chemically different Ni-B distances, namely, Ni-B(6) [B(9)] and Ni-B(5) [B(10)]. The 2.11 Å for Ni-B(5) and 2.18 Å for the chemically equivalent Ni-B(10) distance show the largest deviation from the idealized  $C_{2h}$  symmetry. Although these differences persisted throughout the refinement, the chemical equivalence of these interactions suggested that these differences are not significant; they are within  $3\sigma$  of the mean. The metal-boron distances here fall within the range observed as listed in Table V.<sup>16-24</sup>

The average B-B distance is 1.79 (1) Å. The largest deviation from this average is the B(7)-B(8) distance of 1.97 (2) Å. However, a similar bonding situation occurs in  $B_{10}H_{24}$ <sup>25</sup> where the distance is 2.01 Å. The average terminal B-H distance is 1.22 (5) Å. The average bridging B-H distance is 1.34 (12) Å, but the deviation from the average is large for the distances involving H(67). The distances fall in the observed range of B-H distances.<sup>26</sup> Hydrogen atoms also bridge edge positions of an open pentagonal face in  $B_{11}H_{13}$ <sup>2-</sup> but they are disordered in that structure.<sup>27</sup>

(16) R. M. Wing, *J. Amer. Chem. Soc.*, **89**, 5599 (1967).

(17) R. M. Wing, *ibid.*, **90**, 4828 (1968).

(18) R. M. Wing, *ibid.*, **92**, 1187 (1970).

(19) A. R. Kane, L. J. Guggenberger, and E. L. Muetterties, *ibid.*, **92**, 2571 (1970).

(20) D. St. Clair, A. Zalkin, and D. H. Templeton, *ibid.*, **92**, 1173 (1970).

(21) M. R. Churchill and K. Gold, *ibid.*, **92**, 1180 (1970).

(22) B. G. DeBoer, A. Zalkin, and D. H. Templeton, *Inorg. Chem.*, **7**, 2288 (1968).

(23) D. St. Clair, A. Zalkin, and D. H. Templeton, *ibid.*, **8**, 2080 (1969).

(24) A. Zalkin, T. E. Hopkins, and D. H. Templeton, *ibid.*, **5**, 1189 (1966).

(25) J. S. Kasper, C. M. Lucht, and D. Harker, *Acta Crystallogr.*, **3**, 436 (1950).

(26) W. N. Lipscomb, "Boron Hydrides," W. A. Benjamin, New York, N. Y., 1963.

(27) C. J. Fritchie, *Inorg. Chem.*, **6**, 1199 (1967).

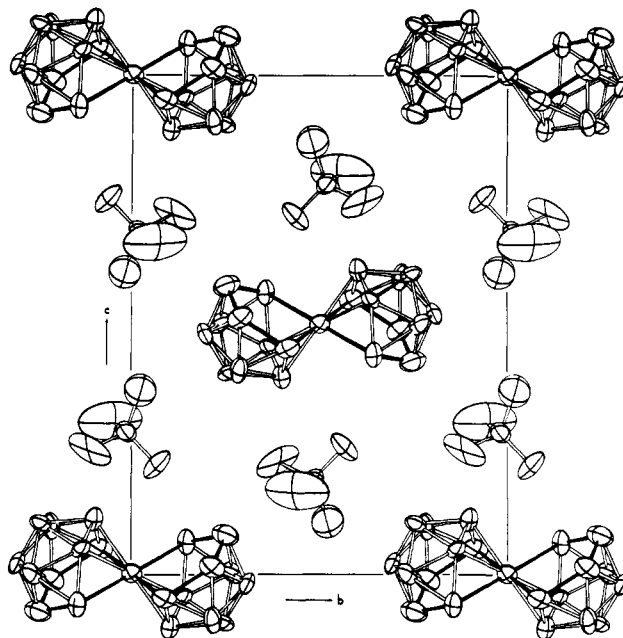


Figure 3. The  $yz$  projection of the crystal structure of  $[(CH_3)_4N]_2Ni(B_{10}H_{12})_2$ .

Table V. M-B Distances in Metalloboranes (Carboranes)<sup>a</sup>

	M-B, Å	Metal configura- tion	Ref
$(Et_4N)_2Cu(B_9C_2H_{11})_2$	2.13	$d^9$	16
$[(CH_3)_4N]_2Ni(B_{10}H_{12})_2$	2.15	$d^8$	
	2.23		
$[(C_6H_5)_3PCH_3]Cu(B_9C_2H_{11})_2$	2.15	$d^8$	17
$[CH_3N(C_2H_4)_3NCH_3][Ni(neo-C_2B_9H_{11})_2]$	2.11 <sup>b</sup>	$d^8$	18
	2.18		
$[(C_2H_5)_3P]Pt(H)B_9H_{10}S$	2.23	$d^8$	19
$Ni(B_9C_2H_{11})_2$	2.12	$d^6$	20
$Ni[(CH_3)_2B_9C_2H_9]_2$	2.11	$d^6$	21
	2.15		
$N(CH_3)_4Co(B_9C_2H_8Br_3)_2$	2.16	$d^6$	22
$Cs_2(B_9C_2H_{11})Co(B_9C_2H_{10})Co(B_9C_2H_{11}) \cdot H_2O$	2.10	$d^6$	23
$Cs(B_9C_2H_{11})Re(CO)_3$	2.35	$d^6$	24

<sup>a</sup> The structures and distances considered in this tabulation are those where the metal-boron geometry is basically ordered and the boron atom is not bonded to any other heteroatom (including carbon). Each boron atom is six coordinate (assuming M-B occupies one coordinate site) and the framework is 12-atom icosahedral or an 11-atom icosahedral fragment. <sup>b</sup> The boron atoms here are also bonded to one carbon atom in exception to the preceding restrictions.

The  $yz$  projection of the crystal structure is shown in Figure 3. The large anisotropic thermal motion of the tetramethylammonium carbon atoms is obvious in Figure 3. All the nonbonding interactions were examined. The shortest nonbonding interactions are given in Table VI. The majority of these contacts are intramolecular contacts between atoms of the two fused polyhedra in the dianion.

The question arises as to the symmetry of the metal ligand interactions in electron-rich metalloboranes (carboranes). The structure of the  $d^8$   $[(C_6H_5)_3PCH_3]Cu(B_9C_2H_{11})_2$ <sup>17</sup> and the  $d^9$   $(Et_4N)_2Cu(B_9C_2H_{11})_2$ <sup>16</sup> have the dicarbollide ligands slipped relative to a symmetric sandwich configuration. However, in the  $d^8$   $[CH_3N(C_2H_4)_3][Ni(neo-C_2B_9H_{11})_2]$  structure there is little or no distortion from a symmetric sandwich structure.<sup>18</sup> All observed transition metal dicarbollide structures

Table VI. Selected Nonbonding Interatomic Distances<sup>a</sup>

B(5)-B(9')	3.09 (2)	H(6)-B(9')	2.80 (10)
B(5)-H(89')	2.99 (12)	H(6)-H(9')	2.39 (13)
B(6)-B(9')	2.88 (2)	H(6)-H(10')	2.49 (13)
B(6)-B(10')	3.13 (2)	H(67)-B(9')	3.14 (11)
B(6)-H(9')	2.88 (10)	H(67)-B(10')	2.75 (11)
B(6)-H(10')	2.82 (10)	H(67)-H(10')	2.13 (13)
H(5)-B(9')	2.92 (9)	H(6)-H(10) <sup>b</sup>	2.06 (13)
H(5)-H(9')	2.90 (13)	C(1)-H(4) <sup>c</sup>	2.86 (10)
H(5)-H(89')	2.48 (14)	C(2)-H(4) <sup>d</sup>	3.00 (9)

<sup>a</sup> The unique contacts for C-C or B-B less than 3.25 Å, C-H or B-H less than 3.00 Å, and H-H less than 2.50 Å. The primed atoms are at  $(-x, -y, -z)$ . <sup>b</sup> Second atom is at  $(x - 1, y, z)$ . <sup>c</sup> Second atom is at  $(1 - x, 1/2 + y, 1/2 - z)$ . <sup>d</sup> Second atom is at  $(x, -1/2 - y, 1/2 + z)$ .

(Table V for some references) with six or fewer d valence electrons have a symmetric sandwich configuration.

The metal-borane geometry in  $[(\text{CH}_3)_4\text{N}]_2\text{Ni}(\text{B}_{10}\text{H}_{12})_2$  is shown in Figure 2. It appears that the metal-borane geometry is the most symmetric possible maintaining maximum metal-boron bonding. The atoms B(5), B(6), B(9), and B(10) are within 0.01 Å of being planar and the nickel atom is 1.42 Å from the resultant best least-squares plane ( $0.2083X + 0.9751Y - 0.7645Z + 1.42$  relative to  $a, b, c^*$ ). The corresponding plane in the other polyhedron [B(5'), B(6'), B(9'), B(10')] is parallel by symmetry. The maximum deviation of the atoms B(1), B(2), B(4), B(7), and B(8) from a plane is 0.03 Å and this plane is tilted  $1.5^\circ$  from the previous plane and displaced by 1.49 Å. Clearly, the decaborane geometry is not very distorted in bonding to the nickel atom.

The geometry observed for  $\text{Ni}(\text{B}_{10}\text{H}_{12})_2^{2-}$  had been predicted earlier, by Klanberg, Wegner, Parshall, and Muettterties.<sup>1</sup> The  $\text{B}_{10}\text{H}_{12}^{2-}$  ligands were described as being formally bidentate complexing to an essentially  $\text{dsp}^2$  square-planar nickel atom. This involves nickel orbitals directed at [B(5)-B(6)] and [B(9)-B(10)] on one cage and the corresponding atoms on the other cage. The angle subtended at the nickel atom from the mid-points of the B(5)-B(6) and B(9)-B(10) bonds is  $80.8^\circ$ . The esr data for  $\text{Co}(\text{B}_{10}\text{H}_{12})_2^{2-}$  makes such a description particularly attractive. The structure observed here holds strictly for  $[(\text{CH}_3)_4\text{N}]_2\text{Ni}(\text{B}_{10}\text{H}_{12})_2$  and the isomorphous  $[(\text{CH}_3)_4\text{N}]_2\text{Co}(\text{B}_{10}\text{H}_{12})_2$ . However, the platinum and palladium complexes probably have this structure by analogy along with supporting spectral data. Also, similar metal-borane interactions are predicted for the  $\text{M}(\text{B}_{10}\text{H}_{12})(\text{PR}_3)_2$  and  $\text{M}(\text{B}_{10}\text{H}_{12})\text{L}_3^-$  complexes.<sup>1</sup> The  $\text{Zn}(\text{B}_{10}\text{H}_{12})_2^{2-}$  structure is different as evidenced by its  $^{11}\text{B}$  nmr spectrum. Tetrahedral coordination of zinc can be accommodated with similar zinc-borane interactions to those observed here by rotating one of the fused polyhedra in Figure 2 by  $90^\circ$  about the Z axis.

**Bonding.** Qualitatively one might view the bonding as arising from the  $\pi$  complexing of nickel by two butadienyl ligands ( $\text{B}_4\text{H}_4^-$ ). The ligand orbitals ( $2A_g + 2B_g + 2A_u + 2B_u$ ) are constructed from linear combinations of p orbitals and are of the proper symmetry to interact with the appropriate metal orbitals ( $4A_g + 2B_g + A_u + 2B_u$ ). The resultant molecular orbitals would depend on the energies and overlaps which cannot be guessed easily.

Molecular orbital (MO) calculations of the LCAO-MO extended Hückel variety<sup>28</sup> were done on  $\text{Ni}(\text{B}_{10}\text{H}_{12})_2^{2-}$ .

The minimum expectation here was to predict the relative atom charge distribution. The atom positions used were those refined in this work averaged to give an anion of  $C_{2h}$  symmetry. The symmetry unique coordinates are listed in Table VII. The local

Table VII. Positional Parameters Used in MO Calculations<sup>a</sup>

Atom	X	Y	Z
B(1)	-1.5713	0.0	2.9191
B(2)	-0.5603	-1.4750	2.9442
B(3)	0.0	0.0	3.7820
B(5)	-1.3142	-0.9404	1.4133
B(6)	0.2767	-1.7039	1.4134
B(7)	1.1311	-0.9888	2.8787
H(1)	-2.4719	0.0	3.3137
H(2)	-0.8201	-2.4765	3.6856
H(3)	0.0	0.0	4.8720
H(5)	-2.1518	-1.4425	0.7476
H(6)	0.5675	-2.8565	1.0654
H(7)	2.0565	-1.5218	3.2933
H(67)	1.3236	-1.1499	1.5806

<sup>a</sup> The coordinates are Cartesian coordinates relative to the axes shown in Figure 2.

coordinate system for the MO calculations is shown in Figure 2. In this coordinate system the metal orbital symmetries are as follows.

$$A_g: 4s, 3d_{x^2 - y^2}, 3d_{z^2}, 3d_{xz}$$

$$B_g: 3d_{xy}, 3d_{yz}$$

$$A_u: 4p_y$$

$$B_u: 4p_x, 4p_z$$

Slater atomic orbitals (AO) were used for the basis set. The nickel atom 4s and 4p orbital exponents were those used by Armstrong, *et al.*,<sup>29</sup> while the 3d exponents were those of the "double- $\zeta$ " form.<sup>30</sup> The boron and hydrogen values were those used earlier.<sup>8</sup> The Coulomb integrals were taken as the negatives of the valence-state ionization potentials and the off-diagonal matrix terms were evaluated using the Wolfsberg-Helmholz<sup>31</sup> approximation of  $H_{ij} = KS_{ij}(H_{ii} + H_{jj})/2$  with  $K = 1.75$ . The nickel  $H_{ii}$  terms were evaluated as a function of charge and electronic configuration in a self-consistent charge iterative procedure.<sup>32</sup> These data are summarized in Table VIII.

Table VIII. Orbital Exponents and Energies

Atom	Orbital	Exponent	$-H_{ii}$ , eV
Nickel	3d	5.75 (0.5683) <sup>a</sup>	14.60 <sup>b</sup>
		2.00 (0.6292)	
Nickel	4s	1.47	11.62
Nickel	4p	1.15	7.41
Boron	2s	1.29	14.90
Boron	2p	1.21	8.42
Hydrogen	1s	1.00	13.60

<sup>a</sup> The numbers in parentheses are coefficients in the "double- $\zeta$ " expansion. <sup>b</sup> The nickel atom energies are the values at the end of the iterative procedure.

(28) (a) R. Hoffmann and W. N. Lipscomb, *J. Chem. Phys.*, **36**, 2179, 3489 (1962); (b) R. Hoffmann, *ibid.*, **39**, 1397 (1963).

(29) A. T. Armstrong, D. G. Carroll, and S. P. McGlynn, *ibid.*, **47**, 1104 (1967).

(30) J. W. Richardson, W. C. Nieuwpoort, R. R. Powell, and W. F. Edgell, *ibid.*, **36**, 1057 (1962).

(31) M. Wolfsberg and L. Helmholz, *J. Chem. Phys.*, **20**, 837 (1952).

(32) C. J. Ballhausen and H. B. Gray, "Molecular Orbital Theory," W. A. Benjamin, New York, N. Y., 1964, Chapter 8.

The calculation resulted in a  ${}^1A_g$  ground state with a gap energy between the highest occupied and lowest unoccupied MO of 3.21 eV. The charge on the nickel atom was 0.16. The final electron configuration of the nickel atom was  $(3d)^{9.61} (4s)^{0.51} (4p)^{-0.28}$ . The  $-0.28$  for  $4p$  is physically impossible. It represents the sum of many antibonding interactions, primarily between the nickel  $4p$  AO's and the boron  $2s$  AO's. The orbital exponents were not altered here, however, since this effect could result from the nature of the Mulliken approximation in the partitioning of electron density.<sup>33</sup> One cannot say that the  $4p$  AO's are not important in bonding since some occupied MO's have appreciable density in these orbitals. Some insight into the nature of the metal-ligand bonding is obtained on examining the overlap populations between the nickel atom and the eight borons to which it bonds. The overlap population subtotals for the nickel AO's are 0.23 for Ni ( $3d$ ), 0.90 for Ni ( $4s$ ), and 0.02 for Ni ( $4p$ ). Clearly the bonding primarily involves the Ni ( $4s$ ) orbital. Examination of individual overlaps shows that the primary nickel bonding to B(5) [B(10)] is between the  $4s$  of Ni and the  $2s$ ,  $2p_x$ , and  $2p_z$  of B(5) in decreasing order of importance. For B(6) [B(9)] it is between  $4s$  of Ni and the  $2s$ ,  $2p_y$ , and  $2p_z$  of B(6) in decreasing order of importance.

The highest occupied and lowest unoccupied MO's are both of  $B_u$  symmetry. Interestingly, the only metal AO's of the proper symmetry to contribute to these MO's are  $4p_x$  and  $4p_z$ . The largest electron density in the highest occupied MO is in the metal  $p_x$  and  $p_z$  AO's and in the ligand  $p_x$  and  $p_z$  AO's of B(5) [B(10)].

(33) R. S. Mulliken, *J. Chem. Phys.*, **23**, 1833, 1841, 2338, 2343 (1955).

This is reflected in the larger overlap population and shorter distance between Ni and B(5). The first unoccupied MO puts the electron density primarily in the metal  $p_x$  (and a smaller amount in  $p_z$ ) and in the ligand  $p_x$  AO of B(6) [B(9)]. The calculations suggest that a two-electron oxidation of the anion would lead to more nearly equal Ni-B bond lengths at the Ni-B(6) distance, whereas a two-electron reduction might lead to more nearly equal lengths at the Ni-B(5) distance.

The ligand displacement in the  $XZ$  plane is a delicate balance between the nature of the metal (which influences the overlap strengths and the number of electrons available) and the nature of the ligand (both symmetry and electron availability are important). Here the symmetry of the molecule forces restrictions on the relative positions of the two fused polyhedra (the mirror plane prohibits movement along the  $Y$  axis). In general, maximizing the metal-ligand overlap (within the molecular symmetry constraints) can lead to slippage of the two polyhedra relative to the metal-ligand axis.<sup>34</sup>

The individual atoms charges are as follows:  $-0.05$  for B(1),  $+0.09$  for B(2),  $+0.10$  for B(3),  $-0.02$  for B(5),  $+0.20$  for B(6),  $+0.17$  for B(7),  $-0.16$  for H(1),  $-0.24$  for H(2),  $-0.18$  for H(3),  $-0.21$  for H(5),  $-0.22$  for H(6),  $-0.19$  for H(7), and  $+0.02$  for H(67). The charges for the other atoms are related to these by the  $C_{2h}$  symmetry operations. The relative charge distribution should not change greatly with parameterization so that these values should be useful in predicting preferred sites of electrophilic or nucleophilic attack on the borane polyhedra.

(34) L. F. Warren and M. F. Hawthorne, *J. Amer. Chem. Soc.*, **90**, 4823 (1968).

## Phosponitrilic Compounds. XII.<sup>1</sup> The Alkaline Hydrolysis of Fluoroalkoxycyclophosphazenes<sup>2</sup>

H. R. Allcock\* and E. J. Walsh

*Contribution from the Department of Chemistry,  
The Pennsylvania State University, University Park, Pennsylvania 16802.  
Received June 5, 1971*

**Abstract:** Product analysis studies of the hydrolysis of  $[\text{NP}(\text{OCH}_2\text{CF}_3)_2]_3$  in basic aqueous methanol revealed a nongeminal pathway for the removal of trifluoroethoxy groups from phosphorus. Kinetic studies of the removal of the first fluoroalkoxy group from  $[\text{NP}(\text{OCH}_2\text{CF}_3)_2]_3$ ,  $[\text{NP}(\text{OCH}_2\text{C}_2\text{F}_5)_2]_3$ ,  $[\text{NP}(\text{OCH}_2\text{C}_3\text{F}_7)_2]_3$ ,  $[\text{NP}(\text{OCH}_2\text{CF}_3)_2]_4$ , and  $[\text{NP}(\text{OCH}_2\text{C}_3\text{F}_7)_2]_4$  in basic 25% aqueous diglyme showed that, for cyclic trimers, the ease of ligand displacement is in the order:  $\text{OCH}_2\text{C}_2\text{F}_5 > \text{OCH}_2\text{CF}_3 > \text{OCH}_2\text{C}_3\text{F}_7$ . Cyclic tetramers hydrolyzed two to four times faster than the appropriate trimers. The mechanistic implications of these results are discussed.

Although the hydrolytic behavior of organophosphazenes (organophosponitriles) is of considerable fundamental and technological interest, very little prior work has been reported in this area. It is known that halocyclophosphazenes, such as  $(\text{NPF}_2)_3$  or  $4$ ,  $(\text{NPCl}_2)_3$  or  $4$ , and  $(\text{NPBr}_2)_3$  or  $4$ , hydrolyze quite rapidly in basic

(1) Part XI: H. R. Allcock and W. J. Birdsall, *Inorg. Chem.*, **10**, 2495 (1971).

(2) A preliminary report of this work was contained in a previous communication: H. R. Allcock and E. J. Walsh, *J. Amer. Chem. Soc.*, **91**, 3102 (1969).

homogeneous media to yield hydroxyphosphazenes,  $[\text{NP}(\text{OH})_2]_3$  or  $4$ , and cyclophosphazanes,  $[\text{HN}(\text{P}(\text{O})\text{OH})_3]_3$  or  $4$ , and eventually phosphates and ammonia.<sup>3-9</sup> When both organo and halogeno groups are present as ligands

(3) F. Seel and J. Langer, *Z. Anorg. Allg. Chem.*, **295**, 316 (1958).

(4) H. N. Stokes, *Amer. Chem. J.*, **18**, 780 (1896).

(5) A. Besson and G. Rosset, *C. R. Acad. Sci.*, **143**, 37 (1906).

(6) R. Schenck and G. Römer, *Chem. Ber.*, **57B**, 1343 (1924).

(7) M. Yokoyama, H. Cho, and M. Sakuma, *Kogyo Kagaku Zasshi*, **66**, 422 (1963).

(8) B. I. Stepanov and G. I. Migachev, *Zavod. Lab.*, **32**, 414 (1966).

(9) M. Becke-Goehring and G. Koch, *Chem. Ber.*, **92**, 1188 (1959).